Interavalanche correlations in the self-organized critical state of a multijunction superconducting quantum interference device

S. L. Ginzburg, M. A. Pustovoit, and N. E. Savitskaya
Petersburg Nuclear Physics Institute, Gatchina, Leningrad District 188350, Russia
(Received 28 February 1997; revised manuscript received 26 September 1997)

A discrete-time model of a two-dimensional lattice of Josephson junctions [multijunction superconducting quantum interference device (SQUID)] equivalent to the Abelian sandpile model with currents as heights was studied by computer simulation. We use various methods of injection of current into the lattice: similar to the real experimental conditions and used previously in sandpile simulations, deterministic and stochastic. For most of these methods the probability density of voltage (an equivalent of avalanche size distribution) demonstrates a universal power-law behavior commonly accepted as the only indicator of self-organized criticality. We found that the characteristics specific for each method of injection are interavalanche correlators. They show quasiperiodic behavior (similar to the bulk-SQUID effect observed in real experiments) for deterministic injection, and ordinary exponential decay for strongly stochastic injection. [S1063-651X(98)05502-0]

PACS number(s): 64.60.Lx, 74.50.+r

I. INTRODUCTION

The decade-old concept of self-organized criticality (SOC) is a subject of growing interest for investigators (see, for instance, [1–5]). This concept can be applied for description of a wide range of dissipative dynamical systems. Such systems during their evolution come to a critical state that reproduces itself in further evolution without exact tuning of external parameters. This state is called the self-organized critical state, differing from the ordinary critical state that appears, for instance, at phase transitions. The SOC concept is quite universal and can be used in such diverse areas of science as geophysics, astrophysics, economics, and condensed matter physics.

Surprisingly, in view of such universality, almost all information on SOC has been obtained by computer simulation. In condensed matter physics experimental data are available only for a pile of sand [6]. Naturally, one should like to see more interesting physical systems that exhibit SOC. On the other hand, the phenomenon of the critical state of a hard second-kind superconductor has been known for a long time (see, e.g., [7,8]). This critical state arises as a result of dynamics of field or current and is self-reproducing. From that point it is very similar to SOC systems; however, in the conventional theory the critical state does not possess a fluctuation spectrum that is inherent to SOC, due to the continuous nature of equations describing the critical state.

It was shown in [9] that the equations for currents in a two-dimensional discrete Josephson lattice with open boundaries are identical to those of the two-dimensional sandpile model and, hence, the former system is in the SOC state. In this case we have an Abelian model with currents as heights. However, there is a substantial difference between dropping of sand to a pile and injection of current in a superconductor, either in real or in model experiment. In the sandpile model all grains are of the same size, so that the system behaves as a cellular automaton. Also, at least one grain could be dropped into any place in a pile, either by random or by deterministic rule. On the contrary, the injection current in a superconductor, being an equivalent of addition of sand, could take any continuous value and could be distributed arbitrarily. In particular, the current might be injected into all lattice sites simultaneously by very small portions, as in real experiments. Hence, a natural question arises about variation of the structure of fluctuations in the SOC state for various regimes of injection, i.e., about the universal nature of fluctuations.

Note that in most of the papers on SOC only the distribution functions of various quantities that describe a single avalanche were studied (call them single-avalanche distribution functions). However, interavalanche distribution functions that describe correlations between quantities in different avalanches are also very important for system description. In the experiments with a real sandpile [6] just the interavalanche fluctuation spectra were studied. The only theoretical paper we know that deals with interavalanche correlators is [10].

In the present work we show that the single-avalanche distribution functions are nearly identical for various methods of injection, i.e., they are universal functions. At the same time the interavalanche correlators differ substantially for different methods; while in some cases the correlators decay rapidly when the difference of avalanche numbers increases, in other cases they oscillate revealing a very slow decay. The latter fact was established in [10] but was not studied in detail.

Therefore we found that the interavalanche correlators *do not possess the property of universality. This situation is very similar to that taking place in physics of second-kind phase transitions, where the static single-time correlators behave universally, while the dynamic ones are very sensitive to system peculiarities.*

The present work consists of four sections. In Sec. II we derive the principal equations for various models of Josephson arrays. In particular, for a two-dimensional (2D) multijunction superconducting quantum interference device(S-QUID) we show that they correspond to the algorithm of sandpile automaton. In Sec. III we study numerically the single-avalanche probability densities and the interavalanche correlators of current and voltage. In Sec. IV we summarize our results.

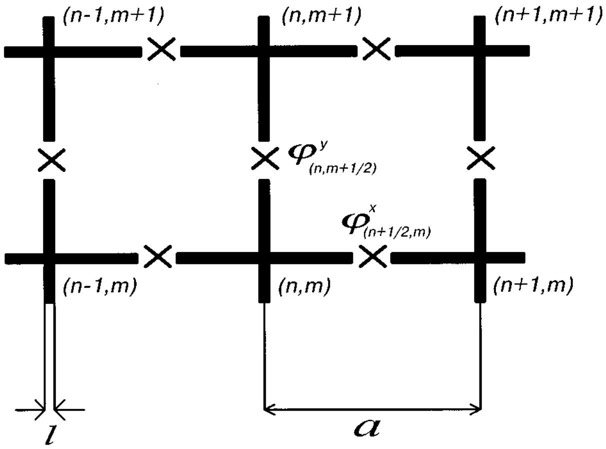

FIG. 1. The 2D Josephson junction array.

II. THE MODEL

In this section we describe the 2D and 3D models of a granular superconductor [Josephson junction array (JJA)] and the 2D model of multijunction SQUID (MJS) [9]. For each of the models we derive the equations for gauge-invariant phase difference $\varphi(t)$. For this derivation we use the resistive model of the Josephson junction [11], where the density of transport current depends on $\varphi(t)$ as

$$j=j_c\sin[\varphi(t)]+\frac{\phi_0}{2\pi\rho_0}\frac{d\varphi(t)}{dt},\tag{1}$$

where j_c is the density of critical current, ϕ_0 is the flux quantum, and ρ_0 is the surface resistivity of the junction.

Further, for the MJS model, making some suggestions that simplify it, we are able to write the equations for junction currents, identical to the rules of addition and toppling in the Abelian sandpile model.

A. Josephson junction array and 2D multijunction SQUID

The 2D granular superconductor can be described as a hollow superconducting system which is infinite in z direction, and its xy section is a square lattice with the lattice constant a (Fig. 1). The lattice ribs are of size l; the Josephson junctions are placed in the middle of each rib. The equations for the gauge-invariant phase difference for such a system have the form

$$\begin{aligned}
j_c\sin(\varphi^x_{n+1/2,m})+\frac{\phi_0}{2\pi\rho_0}\frac{d\varphi^x_{n+1/2,m}}{dt}
&=\frac{\phi_0}{8\pi^2la^2}R^x_{n+1/2,m}(\varphi)+j^{x,(i)}_{n+1/2,m}\\
&=\frac{\phi_0}{8\pi^2la^2}(\varphi^x_{n+1/2,m+1}+\varphi^x_{n+1/2,m-1}-2\varphi^x_{n+1/2,m}\\
&\quad+\varphi^y_{n,m+1/2}-\varphi^y_{n,m-1/2}+\varphi^y_{n+1,m-1/2}-\varphi^y_{n+1,m+1/2})\\
&\quad+j^{x,(i)}_{n+1/2,m},
\end{aligned}\tag{2}$$

$$\begin{aligned}
j_c\sin(\varphi^y_{n,m+1/2})+\frac{\phi_0}{2\pi\rho_0}\frac{d\varphi^y_{n,m+1/2}}{dt}
&=\frac{\phi_0}{8\pi^2la^2}R^y_{n,m+1/2}(\varphi)+j^{y,(i)}_{n,m+1/2}\\
&=\frac{\phi_0}{8\pi^2la^2}(\varphi^y_{n-1,m+1/2}+\varphi^y_{n+1,m+1/2}-2\varphi^y_{n,m+1/2}\\
&\quad+\varphi^x_{n-1/2,m+1}-\varphi^x_{n+1/2,m+1}+\varphi^x_{n+1/2,m}-\varphi^x_{n-1/2,m})\\
&\quad+j^{y,(i)}_{n,m+1/2},
\end{aligned}\tag{3}$$

where $j^{x,(i)}_{n+1/2,m}, j^{y,(i)}_{n,m+1/2}$ are the injection current densities. A similar model was described earlier in [12,13].

Now let us write the 3D generalization of Eqs. (2) and (3). The granular superconductor is now a cubic lattice with the constant a and rib section size $l\times l$, the junctions are still in the middle of the ribs. The equation for the phase difference in the x direction is

$$\begin{aligned}
j_c\sin(\varphi^x_{n+1/2,m,k})+\frac{\phi_0}{2\pi\rho_0}\frac{d\varphi^x_{n+1/2,m,k}}{dt}
&=\frac{\phi_0}{8\pi^2l^2a}R^x_{n+1/2,m,k}(\varphi)+j^{x,(i)}_{n+1/2,m,k}\\
&=\frac{\phi_0}{8\pi^2l^2a}(\varphi^x_{n+1/2,m+1,k}+\varphi^x_{n+1/2,m-1,k}+\varphi^x_{n+1/2,m,k+1}\\
&\quad+\varphi^x_{n+1/2,m,k-1}-4\varphi^x_{n+1/2,m,k}+\varphi^y_{n,m+1/2,k}-\varphi^y_{n,m-1/2,k}\\
&\quad+\varphi^y_{n+1,m-1/2,k}-\varphi^y_{n+1,m+1/2,k}+\varphi^z_{n,m,k+1/2}\\
&\quad+\varphi^z_{n+1,m,k-1/2}-\varphi^z_{n+1,m,k+1/2}-\varphi^z_{n,m,k-1/2})+j^{x,(i)}_{n+1/2,m,k}.
\end{aligned}\tag{4}$$

The phase differences $\varphi^y_{n,m+1/2,k}$, $\varphi^z_{n,m,k+1/2}$ are expressed in the same way. The operators $R^x_{n+1/2,m}$, $R^y_{n,m+1/2}$, $R^x_{n+1/2,m,k}$ are a discrete analog of the operator $-\mathrm{rot}\ \mathrm{rot}(\varphi)$.

In this work we study in detail a different form of the Josephson junction lattice, the 2D multijunction SQUID. Such a SQUID is depicted as two superconducting layers joined by Josephson junctions that are placed in the sites of square lattice of size $L\times L$. The junction size $l\ll a$ (Fig. 2). The Josephson current flows along the z axis.

Thus we can write the following equation for the gauge-invariant phase difference in the junction (n,m):

$$j_c\sin(\varphi_{n,m})+\frac{\phi_0}{2\pi\rho_0}\frac{\partial\varphi_{n,m}}{\partial t}=\frac{\phi_0}{16\pi^2l^2\lambda_L}\Delta_{n,m}(\varphi)+j^{(i)}_{n,m},$$

$$\Delta_{n,m}(\varphi)=\varphi_{n+1,m}+\varphi_{n-1,m}+\varphi_{n,m+1}+\varphi_{n,m-1}-4\varphi_{n,m},\tag{5}$$

where λ_L is the London penetration depth, or, in the dimensionless form,

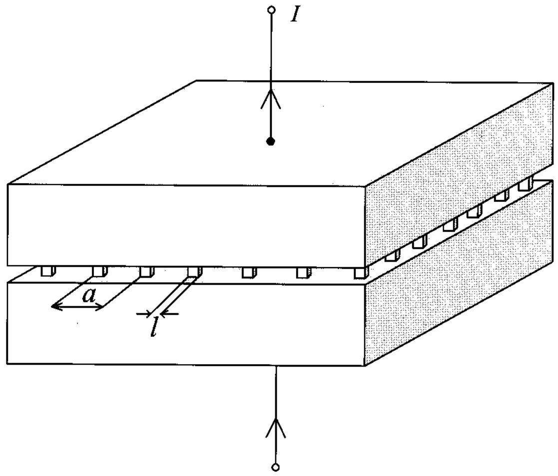

FIG. 2. The 2D multijunction SQUID.

$$V\sin(\varphi_{n,m})+\tau\frac{d\varphi_{n,m}}{dt}=\Delta_{n,m}(\varphi)+2\pi F_{n,m},$$

$$V=2\pi\frac{j_c}{j_\varphi},\quad j_\varphi=\frac{\phi_0}{8\pi l^2\lambda_L},\quad F_{n,m}=\frac{j^{(i)}_{n,m}}{j_\varphi},$$

$$\tau=V\tau_0,\quad \tau_0=\frac{\phi_0}{2\pi\rho_0 j_c}. \tag{6}$$

Here $F_{n,m}$ is the dimensionless injection current.

The parameter V that appears in Eq. (6) is the principal characteristic of the SQUID. For instance, in the case $V\gg1$ the single-junction SQUID has a large (of the order of V) number of metastable states for its energy, and this fact leads to such phenomena as the quantization of magnetic flux and hysteresis [11]. In our model of MJS we consider this case solely.

B. Principal equations

It would be too complicated to solve the system (6) exactly, so we make some simplifications and describe the approximate solution in terms of dimensionless current through the junction $z_{n,m}$:

$$z_{n,m}=z_c\sin(\varphi_{n,m})+\frac{\tau}{2\pi}\frac{d\varphi_{n,m}}{dt},\quad z_c=\frac{V}{2\pi}. \tag{7}$$

In this notation the system (6) looks like

$$z_{n,m}(\varphi)=\frac{1}{2\pi}\Delta_{n,m}(\varphi)+F_{n,m}. \tag{8}$$

Let us simplify Eq. (8), taking into account the properties of the solution of Eq. (7). The latter is an equation for a phase in a single Josephson junction. For $z_{n,m}\leqslant z_c$, we see that the phase is a constant ($d\varphi/dt=0$). For $z_{n,m}>z_c$, however, when $V\gg1$ and $|z_{n,m}-z_c|\ll z_c$, Eq. (7) has a solution $\varphi(t)$ which undergoes only a little change during the time interval T and then varies by 2π during the time $\tau_0\ll T$. We neglect the above mentioned little change (of order of $1/V$) in $\Delta_{n,m}(\varphi)$ and thus approximate the phase by stepwise function

$$\varphi_{n,m}\approx2\pi q_{n,m}+\frac{\pi}{2}, \tag{9}$$

where $q_{n,m}$ is an integer. Using this approximation we rewrite Eqs. (7) and (8) in the form

$$z_{n,m}=z_c\sin(\varphi_{n,m})+\frac{\tau}{2\pi}\frac{d\varphi}{dt},$$

$$z_{n,m}=\Delta_{n,m}(q)+F_{n,m}, \tag{10}$$

$$q_{n,m}=\mathrm{Int}\left(\frac{\varphi_{n,m}}{2\pi}+\frac{1}{4}\right),$$

where $\mathrm{Int}(x)$ denotes an integer part of x.

Equations (10) form a complete system which is simpler than Eq. (5) due to the fact that the phases do not interact. Let us describe the solution of this simplified system. As a first step we trace the evolution of the phase in the junction (n_0,m_0). We choose as initial condition the situation when the injection current for all sites $F_{n,m}=K=\mathrm{Int}(z_c)<z_c$, and the phases in all sites are

$$\varphi_{n,m}(0)=\arcsin\left(\frac{2\pi K}{V}\right)\simeq\frac{\pi}{2}-\sqrt{2\left(1-\frac{2\pi K}{V}\right)}. \tag{11}$$

Then $q_{n,m}=0$ and $\Delta_{n,m}(q)=0$.

Further, let us suppose that the current is injected by integer portions (''quanta''), i.e., $F_{n,m}$ and hence $z_{n,m}$ are integer numbers. Adding in the site (n_0,m_0) a single unit current ($F_{n_0,m_0}=K+1$), we obtain

$$z_{n_0,m_0}\rightarrow z_{n_0,m_0}+1. \tag{12}$$

The current now exceeds the critical value, so $d\varphi_{n_0,m_0}/dt>0$. The solution for φ_{n_0,m_0} can be found from the first Eq. (10). The remarkable property of this solution is that the phase is almost constant during the period $T=2\pi\tau_0/\sqrt{2[(K+1)/z_c-1]}$, and then changes abruptly by 2π during the interval τ_0. At the very moment of phase jump we have

$$\begin{aligned}q_{n,m}&\rightarrow q_{n,m}+1,\\ \Delta_{n,m}&\rightarrow\Delta_{n,m}-4,\\ \Delta_{n\pm1,m}&\rightarrow\Delta_{n\pm1,m}+1,\\ \Delta_{n,m\pm1}&\rightarrow\Delta_{n,m\pm1}+1.\end{aligned} \tag{13}$$

Then z_{n_0,m_0} is changed in accordance with the rules

$$\begin{aligned}z_{n_0,m_0}&\rightarrow z_{n_0,m_0}-4,\\ z_{n_0\pm1,m_0}&\rightarrow z_{n_0\pm1,m_0}+1,\\ z_{n_0,m_0\pm1}&\rightarrow z_{n_0,m_0\pm1}+1.\end{aligned} \tag{14}$$

The rules (12), (14) for z_{n_0,m_0} are completely identical to the rules of addition and toppling in the Abelian sandpile model [1,14], thereby demonstrating that our system is a SOC one.

When turning to the whole lattice the following difficulty appears. The time T of small phase change varies from site to site, and changes also when a jump of phase occurs in any nearest site during this time interval. As Eqs. (10) take this change into account, they remain still too complicated to analyze. Let us make one more simplification. We suppose that T is the same for all sites, thus being able to introduce a discrete time $t_k = Tk$ in our system. We hope that such a simplified model still describes the physical properties of the system correctly. Now we can transform Eq. (10) in equations that include only $q_{n,m}$ and $z_{n,m}$:

$$q_{n,m}(k+1)=q_{n,m}(k)+\theta(z_{n,m}(k)-z_c),$$
$$z_{n,m}(k)=\Delta_{n,m}(q(k))+F_{n,m}(k), \tag{15}$$

then for $z_{n,m}$ we have

$$\begin{aligned} z_{n,m}(k+1)&=z_{n,m}(k)+\Delta_{n,m}\theta(z(k)-z_c)+\xi_{n,m}(k)\\ &=z_{n,m}(k)+\theta(z_{n+1,m}(k)-z_c)+\theta(z_{n-1,m}(k)-z_c)\\ &\quad+\theta(z_{n,m+1}(k)-z_c)+\theta(z_{n,m-1}(k)-z_c)\\ &\quad-4\theta(z_{n,m}(k)-z_c)+\xi_{n,m}(k),\\ &\quad \xi_{n,m}(k)=F_{n,m}(k+1)-F_{n,m}(k). \end{aligned} \tag{16}$$

The behavior of our system is determined also by the statistical properties of noise $\xi_{n,m}$ (see Sec. III below) and by boundary conditions which play an important role in SOC problems.

C. Boundary conditions

In this section we consider the boundary conditions in relation to the physics of our system. The boundary conditions most frequently used in SOC problems are of two kinds: open and closed ones. The open boundaries are realized in our system when the whole lattice is shunted by a normal superconductor with a critical current several orders of magnitude larger than that of the Josephson junction. This means that we add the stripes of junctions with $n,m=0,N+1$ to the lattice $1\leqslant(n,\ m)\leqslant N$ and set their critical current density to infinity:

$$z_c=\infty, \quad n,m=0,\ N+1. \tag{17}$$

The current in these junctions always increases, thus it cannot return to the sublattice $1\leqslant n,m\leqslant N$. In other words, the current is able to leave the lattice, thus realizing the open boundary conditions. The condition (17) is equivalent to

$$z_{n,m}=0, \quad n,m=0,\ N+1 \tag{18}$$

that was used commonly in SOC problems.

Taking Eq. (17) into account, we can modify Eq. (16) for boundary sites, e.g., (1,1) and $(1,m)$:

$$\begin{aligned} z_{1,1}(k+1)&=z_{1,1}(k)+\theta(z_{2,1}(k)-z_c)+\theta(z_{1,2}(k)-z_c)\\ &\quad-4\theta(z_{1,1}(k)-z_c)+\xi_{1,1}(k),\\ z_{1,m}(k+1)&=z_{1,m}(k)+\theta(z_{2,m}(k)-z_c)+\theta(z_{1,m+1}(k)-z_c)\\ &\quad+\theta(z_{1,m-1}(k)-z_c)-4\theta(z_{1,m}(k)-z_c)\\ &\quad+\xi_{1,m}(k). \end{aligned} \tag{19}$$

The closed or reflecting boundary conditions mean that the current cannot leave the system, i.e., that the lattice is surrounded by an insulator. Equations (16) in this case change to

$$\begin{aligned} z_{1,1}(k+1)&=z_{1,1}(k)+\theta(z_{2,1}(k)-z_c)+\theta(z_{1,2}(k)-z_c)\\ &\quad-2\theta(z_{1,1}(k)-z_c)+\xi_{1,1}(k). \end{aligned} \tag{20}$$

The current is conserved in such a system, while for open boundary conditions it is conserved only in the extended lattice $0\leqslant(n,\ m)\leqslant N+1$.

D. Electrodynamics of the system

Equations (16) that describe the dynamics of current in our lattice can be written in a brief form:

$$z_{n,m}(k+1)=z_{n,m}(k)+\Delta_{n,m}\Psi(z(k))+\xi_{n,m}(k),$$
$$\Psi(z(k))=\theta(z-z_c). \tag{21}$$

In this section we consider the physical meaning and possible modifications of $\Psi(z)$. First, let us write the dependence of junction voltage on the phase in it:

$$U_{n,m}(t)=-\frac{\phi_0}{2\pi}\frac{\partial\varphi_{n,m}}{\partial t}. \tag{22}$$

When the junction current exceeds the critical value, the phase changes by 2π during a time interval $T+\tau_0$, and the mean voltage is

$$U_{n,m}(k+1/2)=\frac{1}{T}\int_{t_k}^{t_{k+1}}U_{n,m}(t)dt=-\frac{\phi_0}{T} \tag{23}$$

or, more generally,

$$\begin{aligned} U_{n,m}(k+1/2)&=-\frac{\phi_0}{T}\theta(z_{n,m}(k)-z_c)\\ &=-\frac{\phi_0}{T}[q_{n,m}(k+1)-q_{n,m}(k)]. \end{aligned} \tag{24}$$

Thus, using Eq. (16), we can write

$$z_{n,m}(k+1)-z_{n,m}(k)=-\frac{T}{\phi_0}\Delta_{n,m}(U(k+1/2))+\xi_{n,m}(k). \tag{25}$$

Comparing Eqs. (25) and (21) we see that

$$U_{n,m}(k+1/2)=-\frac{\phi_0}{T}\Psi(z_{n,m}(k)), \tag{26}$$

i.e., $\Psi(z)$ has the physical meaning of the current-voltage characteristic (CVC) of a junction. Consider now some modifications of CVC.

(1) In Eq. (21) we consider only the positive threshold of CVC because of the fact that the current values are always near this threshold. The expression for CVC that takes into account both thresholds is

$$\Psi(z)=\theta(z-z_c)-\theta(-z-z_c). \tag{27}$$

(2) Equation (27) is written for zero temperature. To introduce the temperature in an accurate way would be a rather complicated task; however, one can do this phenomenologically, being guided by simple physical grounds that a nonzero temperature leads to an exponential smearing of threshold in the CVC, as for a single Josephson junction [11]. Following the classical idea of Anderson and Kim [15], we replace $\vartheta(z(k)-z_c)$ by Fermi step:

$$f(z)=\frac{1}{1+\exp[-(z-z_c)/z_0]},$$
$$z_0\ll 1\ll z_c \tag{28}$$

where z_0 is proportional to the temperature. Then $\Psi(z)=f(z)$ for one threshold, and $\Psi(z)=f(z)-f(-z)$ for two ones.

One can obtain some other SOC models by writing Eq. (21) in a more general form and modifying $\Psi(z)$:

$$z_{n,m}(k+1)=z_{n,m}(k)+\Delta^b_{n,m}(\Psi(z(k)))+\xi_{n,m}(k),$$

$$\Delta^b_{n,m}=b\{\Psi(z_{n+1,m})+\Psi(z_{n-1,m})+\Psi(z_{n,m+1})+\Psi(z_{n,m-1})\}-4\Psi(z_{n,m}). \tag{29}$$

Then, for $\Psi(z)=\frac{1}{4}z\theta(z-z_c)$ and $b=1$ we obtain the model that was used in [16], and for $0<b<1$ we have a nonconservative model used in [17,18].

III. COMPUTER SIMULATION RESULTS

All our simulations were performed for the square lattice of size $L\times L$ $(L=23)$, open boundary conditions, and $z_c=4.5$, $z_0=0$. We made our simulations in the following way.

First, an initial configuration with random noninteger $z_{n,m}$ varying from 0 to z_c is prepared.

Next, in Eq. (16) we take $\xi_{n,m}\neq 0$, according to one of the methods described below, thus launching the dynamic process. Until the dynamics stops (i.e., the system reaches a metastable state), we keep $\xi_{n,m}=0$. Then we add a nonzero $\xi_{n,m}$ again and so on.

We call ''an avalanche'' the process of single addition and further relaxation of the system. For every avalanche the following quantities are defined: (1)

$$z_j=\frac{1}{N}\sum_{n,m} z_{n,m}(k_j), \tag{30}$$

where $N=L^2$ and k_j is the final moment of the jth avalanche. The quantity Nz_j is the total current in a lattice and it corresponds to the total mass of a pile in the Abelian sandpile model (see, e.g., [10]). (2)

$$u_j=\frac{1}{N}\sum_{k=k_{j-1}+1}^{k_j}\sum_{n,m}\vartheta(z_{n,m}(k)-z_c). \tag{31}$$

The quantity Nu_j is the total avalanche voltage and it corresponds to the total number of topplings in the jth avalanche.

In Eqs. (30) and (31) we defined two random variables that characterize our process. All our calculations are performed after reaching the stationary critical state. For such a state the following quantities are defined.

(1) Single-avalanche probability densities of current and voltage:

$$\rho(z)=\langle\delta(z-z_j)\rangle,$$
$$\rho(u)=\langle\delta(u-u_j)\rangle. \tag{32}$$

(2) Interavalanche correlators of current and voltage:

$$D_z(j)=\langle z_{j_0}z_{j_0+j}\rangle-\langle z\rangle^2,$$
$$D_u(j)=\langle u_{j_0}u_{j_0+j}\rangle-\langle u\rangle^2. \tag{33}$$

(3) Spectral densities of current and voltage:

$$S_z(\nu)=2\sum_{j=-\infty}^{\infty}D_z(j)e^{-i2\pi\nu j},$$
$$S_u(\nu)=2\sum_{j=-\infty}^{\infty}D_u(j)e^{-i2\pi\nu j}. \tag{34}$$

For real calculations we use the common formulas [19]

$$\rho(z_j)=\frac{N_j}{MW},$$
$$\tilde{z}_j=z_j-\langle z\rangle,$$
$$D_z(j)=\frac{1}{M-j}\sum_{j_0=1}^{M-j}[\tilde{z}_{j_0}\tilde{z}_{j_0+j}],$$
$$S_z(\nu)=\frac{2}{M}\langle|Z_\nu|^2\rangle,$$
$$Z_\nu=\sum_{j=1}^{M}\tilde{z}_je^{-i2\pi\nu j}, \tag{35}$$

where N_j is the number of values of z belonging to the interval $(z_j\pm W/2)$, M is the total number of points in series z_j, u_j, and the angle brackets denote an ensemble average. Expressions for voltage are written in the same way. Note that Eqs. (33)–(35) for ergodic systems lead to identical results when $j\ll M$. In our calculations this condition is always valid.

In the present work we consider four different methods of injection of current into the lattice.

(1) An injection of a unit current into an arbitrary lattice site:

$$\xi_{n,m}=\delta_{n,n_0}\delta_{m,m_0}, \tag{36}$$

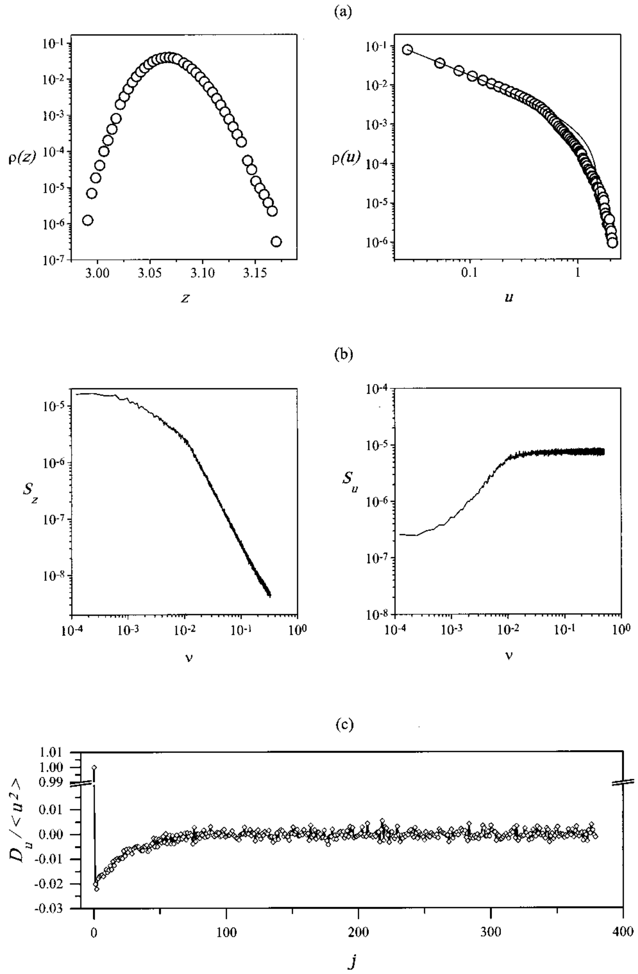

FIG. 3. Results for the first method of injection: (a) probability densities of current $\rho(z)$ and voltage $\rho(u)$ [the curve represents dependence $\rho(u) \sim u^{-1.1}$], (b) power spectra of current $S_z(\nu)$ and voltage $S_u(\nu)$, (c) voltage correlator $D_u(j)$.

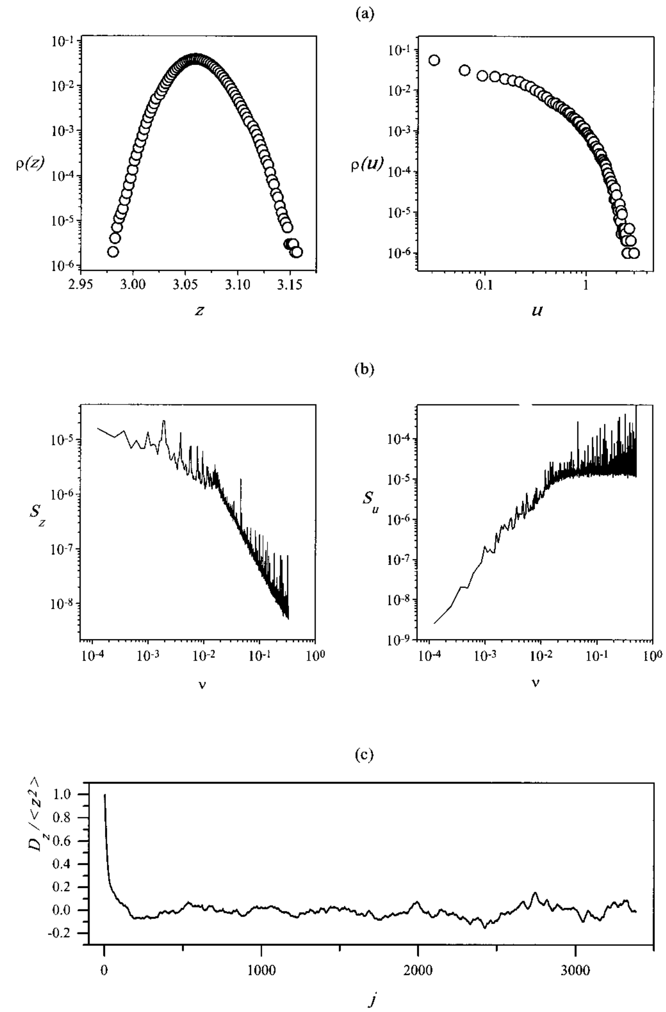

FIG. 4. Results for the second method of injection: (a), (b) the same as in Fig. 3; (c) correlator of current $D_z(j)$.

where (n_0, m_0) is the randomly chosen site. This method is widely used in simulations of the Abelian sandpile model. The results of our calculations are presented in Fig. 3.

We see that the probability density for voltage $\rho(u)$ that corresponds to the cluster-size distribution in the sandpile problem demonstrates standard power-law behavior. The spectrum of current shows a Lorenz-like dependence, i.e., corresponding correlator decays exponentially. The voltage spectrum is of different type. The main power concentrates within the high-frequency range, which corresponds to anticorrelations in $D_u(j)$, clearly seen in Fig. 3(c). [We note that for all the cases described below $S_u(\nu)$ also increases at high frequency.]

(2) Deterministic injection of a unit current into the center of the lattice:

$$\xi_{n,m} = \delta_{n,n_c} \delta_{m,m_c}, \tag{37}$$

where (n_c, m_c) is the central site. This method is known as the ''central seed model'' [10]. The results are presented in Fig. 4. The probability densities of current and voltage demonstrate the same behavior as in the previous case. At the same time the weak peaks appear in $S_z(\nu)$ and $S_u(\nu)$ at frequency $\nu = 1/N$, thus indicating a quasiperiodic process in the system. The correlator $D_z(j)$ also demonstrates a quasiperiodic behavior.

It should be noted that in cases (1) and (2) we used both the random initial configuration described above and the ''empty lattice'' configuration with all $z_{n,m} = 0$ that is common for simulations of the Abelian sandpile model. For both configurations the results were the same.

Besides methods (1) and (2) used earlier in the Abelian sandpile model, we consider some other methods of current injection appearing naturally in our problem.

(3) Deterministic injection of the same arbitrary value of current into all lattice sites:

$$\xi_{n,m} = p. \tag{38}$$

In the methods described above a single unit current was added to the system after every avalanche. Now the total amount of current added at one step is equal to Np, i.e., it is arbitrary. Such a method of injection is typical for experiments with real physical systems. Results for $p = 0.002$ $(Np \approx 1)$ are shown in Fig. 5. It is important that the initial lattice configuration is random. We see that the behavior of single-avalanche probability densities is the same as in cases

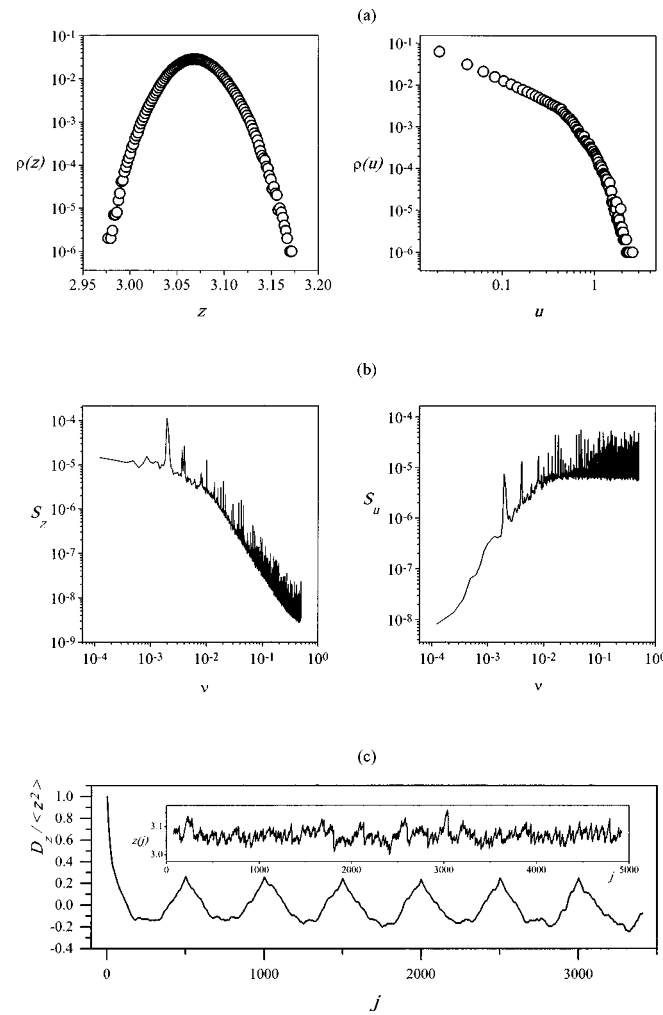

FIG. 5. Results for the third method of injection, $p=0.002$: (a), (b) the same as in Fig. 3, (c) main graph: correlator of current $D_z(j)$; inset: fragment of series of current z_j.

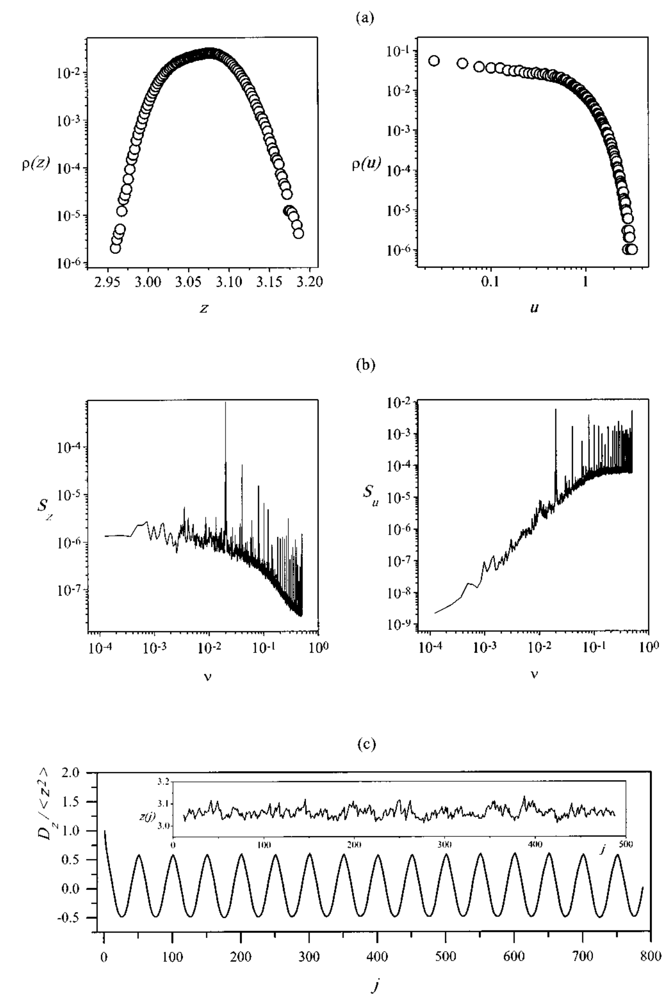

FIG. 6. The same as in Fig. 5 but for $p=0.02$.

(1) and (2). Meanwhile, the spectral densities of current and voltage show pronounced peaks at frequency $\nu\approx p$. The correlator $D_z(j)$ also manifests the presence of a noisy periodic process with the period $T\approx p^{-1}$. At the same time we cannot see any periodicity in the series itself due to large amplitude of noise.

Figure 6 displays the same case but with $p=0.02$ (the total amount of injected current is about 10). The periodicity with $T\approx p^{-1}$ is more distinct. We observed in our simulations that the process is more periodic also in the case of ''smooth'' initial configuration, i.e., when the range of initial current values is taken to be less than $(0\,\ldots\,z_c)$. This fact is a subject of further study.

Thus the correlators in our system oscillate [Figs. 5(c), 6(c)] without any detectable decay. Such a case is a nontrivial one regarding its ergodicity. It can be shown [20] that

$$\frac{1}{M}\sum_{j=1}^{M} z_j \xrightarrow{M\to\infty} \langle z\rangle, \tag{39}$$

when

$$\frac{1}{M}\sum_{j=1}^{M} D_z(j) \xrightarrow{M\to\infty} 0. \tag{40}$$

An oscillating correlator satisfies the latter condition and therefore our system possesses a first order ergodicity. However, time and ensemble averages for correlators are identical only when

$$\frac{1}{M}\sum_{j=1}^{M} D_z^2(j) \xrightarrow{M\to\infty} 0. \tag{41}$$

The condition (41) is not valid for oscillating correlator without decay. Hence, we have only an ergodicity of first order.

(4) An injection of current p into every of R randomly chosen sites, where $R=(1-c)N$. This is equivalent to a random injection into all sites with the distribution

$$P(\xi)=(1-c)\delta(\xi-p)+c\,\delta(\xi), \tag{42}$$

and $\langle\xi\rangle=(1-c)p$. Note that method (3) is the special case of method (4) at $c=0$. The results for $c=1/2$ and $p=1/(1-c)N$ are shown in Fig. 7. We see that for stochastic injection the periodic behavior of the system is suppressed by

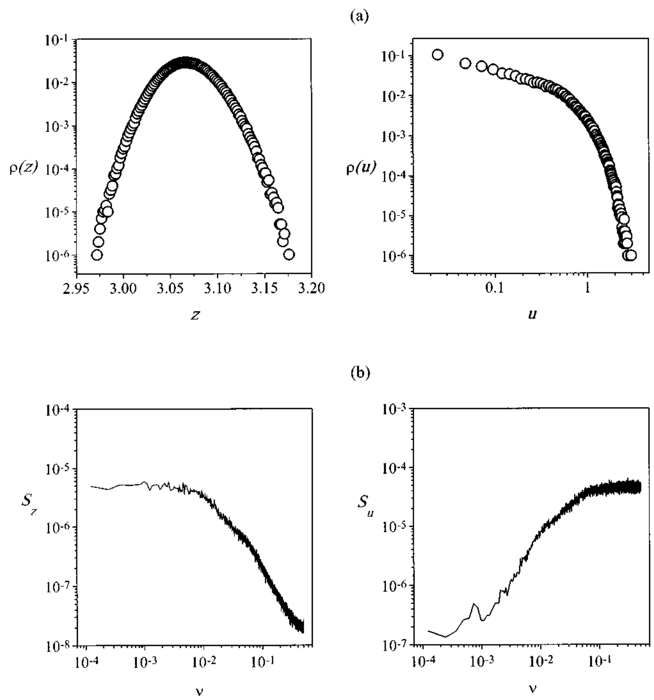

FIG. 7. Results for the fourth method of injection, $c=0.5$, $p=1/N(1-c)$.

noise (note that single-avalanche probability densities show the same behavior as in the cases discussed above).

We conclude that the system behaves quasiperiodically in most of the cases considered, besides the highly stochastic regimes of injection.

IV. SUMMARY

We consider the model of a 2D multijunction SQUID with discrete time. The equations that describe the dynamics of such a lattice are equivalent, for some regimes of current injection, to those of the Abelian sandpile model. This allows us to consider the dynamics of our system in terms of avalanches. In the present work we study interavalanche correlators of both the lattice-averaged current in the final moment of an avalanche and the lattice-averaged total voltage in an avalanche. We consider various methods of current injection, both used earlier in the Abelian sandpile problem as well as similar to experimental ones. The results can be summarized as follows.

(1) Single-avalanche probability densities for current $\rho(z)$ and voltage $\rho(u)$ are nearly identical for all the injection methods we consider, i.e., they are universal functions. Since the power-law behavior of $\rho(u)$ is known as the principal criterion of self-organized criticality, our system demonstrates self-organization in most of the cases considered.

(2) For different injection methods interavalanche correlators behave quite differently. For more or less deterministic injection the system exhibits a quasiperiodic behavior. In fact, our multijunction SQUID works like a single dc SQUID. Such a phenomenon was observed experimentally [21] but is still lacking of an adequate description. For strongly stochastic injection, corresponding, for example, to the random seed model in the sandpile problem, an ordinary exponential decay of correlators is found.

(3) For the voltage, which is an equivalent of the total number of topplings in an avalanche, we observe negative correlations for neighboring avalanches.

ACKNOWLEDGMENTS

The authors are grateful to Dr. V. I. Sbitnev for helpful discussions and to Dr. A. G. Yashenkin and Dr. S. M. Bezrukov for a critical reading of the manuscript. This work has been supported by the Scientific Council on the Problem of High-Temperature Superconductivity and has been performed within the framework of Project Nos. 93050 ''Self-Organized Criticality'' and 96021 ''Profile'' of the State Program on High-Temperature Superconductivity. The work has also been supported by the State program on Physics of Quantum and Wave Processes, subprogram ''Statistical physics,'' Project No. VIII-3, and by the Scientific Council of the State Program ''Neutron Research of Matter.''

[1] P. Bak, C. Tang, and K. Wiesenfeld, Phys. Rev. Lett. **59**, 381 (1987).
[2] P. Bak, C. Tang, and K. Wiesenfeld, Phys. Rev. A **38**, 364 (1988).
[3] C. Tang and P. Bak, Phys. Rev. Lett. **60**, 2347 (1988).
[4] C. Tang and P. Bak, J. Stat. Phys. **51**, 797 (1988).
[5] P. Bak, Physica A **191**, 41 (1992).
[6] G. A. Held, D. H. Solina, D. T. Keane, W. J. Haag, P. M. Horn, and G. Grinstein, Phys. Rev. Lett. **65**, 1120 (1990).
[7] C. P. Bean, Rev. Mod. Phys. **36**, 31 (1964).
[8] A. M. Campbell and J. E. Evetts, *Critical Currents in Superconductors* (Taylor and Francis, London, 1972).
[9] S. L. Ginzburg, Zh. Éksp. Teor. Fiz. **106**, 607 (1994) [JETP **79**, 334 (1994)].
[10] S. S. Manna and J. Kertesz, Physica A **173**, 49 (1991).
[11] A. Barone and G. Paterno, *Physics and Applications of the Josephson Effect* (Wiley, New York, 1982).
[12] T. Wolf and A. Majhofer, Phys. Rev. B **47**, 5383 (1993).
[13] D.-X. Chen, J. J. Moreno, and A. Hernando, Phys. Rev. B **53**, 6579 (1996).
[14] D. Dhar, Phys. Rev. Lett. **64**, 1613 (1990).
[15] P. W. Anderson and Y. B. Kim, Rev. Mod. Phys. **36**, 39 (1964).
[16] Y.-C. Zhang, Phys. Rev. Lett. **63**, 470 (1989).
[17] Z. Olami, H. J. S. Feder, and K. Christensen, Phys. Rev. Lett. **68**, 1244 (1992).
[18] K. Christensen, Z. Olami, and P. Bak, Phys. Rev. Lett. **68**, 2417 (1992).
[19] J. S. Bendat and A. G. Piersol, *Random Data: Analysis and Measurement Procedures* (Wiley, New York, 1986).
[20] S. M. Rytov, *Introduction to Statistical Radiophysics* (Mir, Moscow, 1976) (in Russian).
[21] C. E. Gough, Physica C **153-155**, 1569 (1988).